Electron-impact cross-sections of atmospherically relevant amines from intermediate to 5000 eV energy range

ANAND BHARADVAJA[1] [iD],*, SAVINDER KAUR[2] and K L BALUJA[3]

[1]Department of Physics, Bhaskaracharya College of Applied Sciences, University of Delhi, New Delhi 110 075, India
[2]Department of Physics, SGTB Khalsa College, University of Delhi, Delhi 110 007, India
[3]Formerly at Department of Physics and Astrophysics, University of Delhi, Delhi 110 007, India
*Corresponding author. E-mail: anand_bharadvaja@yahoo.com

Abstract. The amines are major source of environment pollutants emitted in atmosphere from various anthropogenic sources. The non-thermal plasma (NTP)-based technology has proved successful in controlling the emitted amines reaching the atmosphere. The efficient NTP reactors rely on accurate electron–molecule collision data. The electron impact cross-sections are thus obtained for a few amines from ionisation threshold to 5000 eV using the single centre expansion (SCE) formalism. The molecular wave function of each target is obtained from the multicentre expansion of the Gaussian-type orbitals within a single determinant Hartree–Fock self-consistent field scheme. The expansion of wave function, density and potential is carried out at the centre of mass of the molecules. The interaction potential included to model the electron interaction in the target comprises static, correlation-polarisation and exchange types of potentials. The elastic cross-sections are obtained after solving the coupled scattering equations using Volterra integral form. The inelastic effects contributing to electron–molecule scattering are approximated by the ionisation cross-sections. The total cross-sections obtained after summing the elastic and ionisation cross-sections are in good agreement with the available data. We have also tried to explain the effect of polarisation potential on scattering cross-sections. A semiempirical formula based on the spatial extent of the molecule is proposed to estimate the cross-sections for the homologous series of amine molecules.

1. Introduction

The amines are close relatives of NH_3 where the H atom is replaced one at a time by a hydrocarbon group. They fall into different classes depending upon the number of H atoms that have been replaced. The primary and aromatic amines are some of the most abundant amines in atmosphere. They enter the environment through various anthropogenic sources like fossil fuel combustion, automobile exhaust fumes, vulcanisation fumes, industrial gases and dyes [1,2]. These volatile organic compounds (VOC) [3–5] are of major environmental [2,6,7] and health concerns [8–11]. The gas-phase amines on reaction with atmospheric oxidants like O_3 and NO_x produce organic aerosols [12]. Thus, the challenge before scientific community is to have an efficient technology that can control these malodorous gases entering the environment in order to provide clean and safe habitat to live in.

The electron-driven non-thermal plasma (NTP) technology has proved useful in the removal of low-concentration VOC and amines like trimethylamine (TMA) [13–15] and dimethylamine (DMA) [16] even at low temperature [17,18]. The efficient designing of plasma reactors requires in-depth knowledge of electron–molecule collision dynamics. This essentially means that accurate scattering cross-section data are

---

Electronic supplementary material: The online version of this article (https://doi.org/10.1007/s12043-020-1923-z) contains supplementary material, which is available to authorized users.

desired over large electron impact energies. The present collision study also assumes importance in astrophysics as methylamine (MA) and ethylamine (EA) [19–22] are considered as the building blocks of amino acids [23–25]. The presence of these species in astrophysical environment can provide vital clues leading to the origin of life.

The electron-impact scattering cross-sections are presently available only for a few amines like MA [26–29], TMA [29,30], DMA [29,31] and aniline [32]. We have obtained electron-impact elastic cross-sections (ECS) beyond the ionisation threshold upto 5 keV using the single centre expansion (SCE) formalism for various homologous series of amines like methyl-, ethyl-, propyl-, butyl-amine; di- and tri-methylamine and di- and tri-ethylamine. We have also studied the aromatic molecule aniline. These data would be beneficial in devising efficient plasma reactors. In the chosen energy range, inelastic effects contribute significantly to the scattering process. These elastic and inelastic cross-sections are summed incoherently to obtain the total scattering cross-sections (TCS). The working methodology is explained in §2. The collision study from homologous family of molecules has helped in formulating a simple relationship between the TCS belonging to any two members in terms of target parameters. Additionally, we have investigated the effect of polarisation on TCS. An interesting observation is made about the results obtained using the R-matrix and SCE method near the ionisation threshold.

1.1 *SCE method and scattering equations*

In the SCE method [33,34], a three-dimensional quantity like a wave function (bound or continuum), density or potential is reduced to one dimension by expanding it around a single centre in terms of symmetry adapted functions $X_{lh}^{p\mu}(\theta, \phi)$ as

$$G^i(\vec{r}) = \frac{1}{r} \sum_{l,h} G_{i,hl}^{p\mu}(r) X_{hl}^{i,p\mu}(\theta, \phi). \tag{1}$$

The single centre is usually taken as the centre of mass (c.o.m.) of N electron target system. In the above expansion, $G^{p\mu}$ can be either a wave function or electron density. Indices like μ refer to an irreducible representation (IR) for a particular type of point group in the ground state, h denotes a specific basis for a given partial wave l for μ, i is the specific multicentre orbital contributing to the density of bound electrons and r is the distance from the c.o.m. of the molecule. $X_{lh}^{p\mu}(\theta, \phi)$ satisfy orthonormality conditions and for any closed shell molecule in its ground state, the symmetry-adapted functions can

be expressed as a linear combination of real spherical harmonics $S_{lm}(\theta, \phi)$:

$$X_{lh}^{p\mu}(\theta, \phi) = \sum_{m=-l}^{+l} b_{lhm}^{p\mu}(r) S_{lm}(\theta, \phi). \tag{2}$$

b_{lhm} corresponding to a particular IR can be obtained using the character table.

The total interacting potential $V(r)$ is taken as the sum of static (V_{st}), correlation-polarisation (V_{cp}) and exchange (V_{ex}) type of potentials. The static potential is the sum of attractive interaction between the scattering electron and the nuclei as well as the mean-field repulsion with the bound electrons. It is expressed as

$$V_{st}(\vec{r}) = -\int \rho(\vec{s}) \frac{1}{|\vec{r} - \vec{s}|} \, ds + \sum_i^N \frac{Z_i}{|\vec{r} - \vec{R}_i|}. \tag{3}$$

r_i and R_i refer to the space coordinates of the target and the nuclei respectively and ρ is the one-electron density function and is obtained from the bound-state wave function. The summation in the second term is carried over N atoms.

The exchange potential which accounts for the indistinguishability of incident electron and target electrons is represented by Hara-type model potential [35]

$$V_{ex}(\vec{r}) = -\frac{2}{\pi} K_F(\vec{r}) \left[\frac{1}{2} + \frac{1 - \eta^2}{4\eta} \ln \left| \frac{1 + \eta}{1 - \eta} \right| \right], \tag{4}$$

where

$$K_F(\vec{r}) = [3\pi^2 \rho(\vec{r})]^{1/3} \quad \text{and} \quad \eta = k/K_F.$$

The local momentum k is given by

$$k(\vec{r}) = [2(E_{col} + I_P) + K_F^2(\vec{r})]^{1/2}. \tag{5}$$

Here, I_P is the ionisation potential for the neutral target molecule and the collision energy $E_{col} = k_0^2/2$.

The correlation-polarisation potential (V_{cp}) represents the dynamical response of the target to the impinging electron. It includes both the long- and short-range interactions. These interactions are matched smoothly by an analytic expression given by the perturbative expansion of the dipole polarisation forces of the target molecule. V_{cp} is described as

$$V_{cp}(\vec{r}) = \begin{cases} V_{corr}(\vec{r}) & \text{for } r \le r_o \\ V_{pol}(\vec{r}) & \text{for } r > r_o \end{cases} \tag{6}$$

where r_o is the connecting spatial factor obtained from the crossing between the lower polarisation potential terms and the ones given by the correlation potential. V_{corr} given by Perdew and Zunger [36] is used in the

present calculations which is

$$V_{\text{corr}}(\vec{r}) = \begin{cases} (0.0311 + 0.00133 r_s) \\ \quad * \ln r_s - 0.0084 r_s - 0.0584 \text{ for } r_s < 1.0 \\ \dfrac{\gamma \left(1 + \dfrac{7}{6}\beta_1 r_s^{1/2} + \dfrac{4}{3}\beta_2 r_s\right)}{\left(1 + \beta_1 r_s^{1/2} + \beta_2 r_s\right)^2} \text{ for } r_s \geq 1.0 \end{cases}$$

(7)

where $\gamma = -0.1423$ and $\beta_1 = 1.0529$ and $\beta_2 = 0.3334$. V_{pol} is of the form

$$V_{\text{pol}}(\vec{r}) = -\frac{1}{2r^6} \sum_{i,j} x_i x_j \alpha_{ij},$$

(8)

where $r^2 = x_1^2 + x_2^2 + x_3^2$ and α_{ij} is the polarisability tensor.

The interacting potential in an expanded form can be written as

$$V(\vec{r}) = \sum_{lm} V_{lm}(r) X_{lm}^{p\mu}(\theta, \phi).$$

(9)

Having obtained the total interacting potential, the coupled radial integro-differential equations are obtained from the Schrödinger equation for evaluating the radial coefficients for $(N+1)$th continuum electron:

$$\left[\frac{d^2}{dr^2} - \frac{l(l+1)}{r^2} + k_0^2\right] F_{lh}^{p\mu}(r)$$
$$= 2 \sum_{l'h'} V_{lh,l'h'}^{p\mu}(r) F_{l'h'}^{p\mu}(r),$$

(10)

where $k_0^2/2$ is the collision energy. The local potential coupling element $V_{lh,l'h'}(r)$ is given by

$$V_{lh,l'h'}^{p\mu}(r) = \langle X_{lh}^{p\mu}(\hat{r}) | V(\vec{r}) | X_{l'h'}^{p\mu}(\hat{r})\rangle$$
$$= \int d\hat{r} \, X_{lh}^{p\mu}(\hat{r}) V(\vec{r}) X_{l'h'}^{p\mu}(\hat{r}).$$

(11)

Equation (10) is solved under the boundary conditions where the asymptotic form of $F_{lh}^{l'h'}$ is represented as a sum of the incident plane wave of the projectile and the outgoing spherical wave. This generates the necessary K-matrix elements which further allows us to calculate the necessary scattering parameters like S- and T-matrices from where the elastic integral cross-sections (Q_e) can be obtained. The prospective readers may refer to [33,37,38] where numerical procedure employed to solve eq. (10) is given.

$$\sigma_E = \frac{\pi}{k^2} \sum_{lh} \sum_{l'h'} |T_{lh,h'l'}|^2.$$

(12)

A good account of SCE theory is outlined by Sanna and Gianturco [39]. This method has been successfully applied to study the low-energy electron scattering from many molecules by Gianturco group. Some of the past studies are mentioned in the SCE references cited above and in [40,41] to name a few.

1.2 *Ionisation cross-section*

It is well known that at energies beyond ionisation, threshold ionisation process contributes to e^--molecule scattering cross-section appreciably. The non-relativistic ionisation cross-sections are obtained using the binary-encounter-Bethe (BEB) method [42]. The BEB cross-section for an individual molecular orbital i for $E > B$ is given by

$$Q_i(t_i) = \frac{S}{t_i + u_i + 1}$$
$$\times \left[\frac{1}{2}\left(1 - \frac{1}{t_i^2}\right)\ln t_i + 1 - \frac{1}{t_i} - \frac{\ln t_i}{t_i + 1}\right].$$

(13)

The BEB cross-sections are then obtained by summing the individual cross-sections over the occupied molecular orbitals

$$\sigma_I(t) = \sum_i^N Q_i(t_i),$$

(14)

where $t_i = E/B_i$, $u_i = U_i/B_i$ are the normalised energies, $S = 4\pi a_0^2 N_i (R/B_i)^2$. R, B_i, U_i refer to the Rydberg energy, binding energy and orbital kinetic energy respectively of the ith orbital and a_0 is the Bohr's radius. N_i is the orbital occupation number of the ith orbital.

2. Target description and computational details

The molecules we have considered belong to different point group symmetries. These molecules show substantial variation in geometrical size, i.e., electron number, molecular dipole moment and polarisability among themselves. All molecules except for TEA are studied in their natural point group. The target and scattering calculations for TEA are done in C_1 point group instead of C_3 due to restrictions imposed by SCELib [43]. The optimised bound-state molecular wave functions were generated using GAUSSIAN 03 [44] deploying the 6-311G* basis sets. The SCELiB [43] was then used to obtain electron density and potentials. The upper limit of l parameter as defined in eq. (1) for bound-state wave functions was kept sufficiently large (around 50) to ensure a good convergence of molecular properties. This resulted in normalised molecular orbitals ranging between 0.8 and 0.99 for different targets. A very

Table 1. Target parameters of the amines.

Molecule (Name and its formula)	Point group	$\langle R^2 \rangle$ (a.u.)	Number of electrons (N)	Dipole moment (D)	Polarisability[a] (a_0^3)
CH_3NH_2 Methylamine	C_s	94.204	18	1.51 (1.30)[a]	25.30
$CH_3CH_2NH_2$ Ethylamine	C_s	209.712	26	1.37 (1.22)[a]	39.60
$CH_3CH_2CH_2NH_2$ Propylamine	C_s	403.690	34	1.37 (1.17)[a]	51.96
$CH_3(CH_2)_3NH_2$ Butylamine	C_s	692.943	42	1.67 (1.50)[a]	91.22
$(CH_3)_2NH$ Dimethylamine	C_s	203.126	26	1.05 (1.03)[a]	36.76
$C_2H_5)_2NH$ Diethylamine	C_s	666.481	42	0.95 (0.92)[a]	69.20
$(CH_3)_3N$ Trimethylamine	C_{3v}	336.194	34	0.75 (0.61)[a]	47.75
$(CH_3CH_2)_3N$ Triethylamine	C_1	1020.333	58	0.61 (0.69)[a]	90.30
$C_6H_5NH_2$ Aniline	C_s	679.114	50	1.71 (1.53)[a]	78.00

[a]Experimental value [58,59].

fine radial step was used for integration. The quadrature grid was varied in such a way that the normalised wave functions yielded correct value of total number of electrons and dipole moment for each target. This formed an important check to assess the quality of the wave function generated. In calculating the exchange potential, the correlation energy is replaced by ionisation energy. Once the wave function is obtained, the scattering equations were solved numerically to obtain ECS in static-exchange-polarisation (SEP) and static-exchange (SE) models using POLYDCS code [45]. The HF value of the dipole moment of each target is close to its experimental value (denoted in parenthesis). This is summarised in table 1.

3. Result and discussion

Vinodkumar *et al* [28], Shi *et al* [29], Szmytkowski *et al* [30] and Antony *et al* [32] have invoked additivity rule to obtain TCS for molecules like MA, DMA, TMA and aniline. Shi *et al* [29] modified the approach of Jiang *et al* [46] to obtain TCS for electron scattering from MA, TMA and DMA in the energy range from 30 to 5000 eV. Their results are favourable above 100 eV when compared with the experimental data. Vinodkumar *et al* [28] and Antony *et al* [32] have obtained inelastic and total cross-sections for MA and aniline respectively using the multiscattering centre spherical complex optical potential approach. They extracted the total ionisation cross-sections from total cross-sections. It is pertinent to comment that Vinodkumar *et al* [28], Shi *et al* [29] and Antony *et al* [32] have used old form of absorption potential given by Staszewska [47] which was later corrected by Blanco and García [48]. Szmytkowski *et al* [26] determined TCS experimentally for MA from 0.7 to 250 eV energy range. Their other group obtained TCS experimentally and theoretically for TMA [30]. Możejko *et al* [31] theoretically studied elastic electron scattering from DMA in the energy range

from 30 to 3 keV. The digitalised data of Szmytkowski referred by Shi *et al* for DMA may have numerical inaccuracies.

The ECS (σ_E) and BEB (σ_I) cross-sections are computed using the theory as explained earlier. The TCS (σ_T) is approximated by the sum of σ_E and σ_I. This seems to be justified as we have observed in several case studies that the magnitude of electronic excitation cross-sections is small in comparison to ionisation cross-sections beyond the ionisation threshold [49–52] and this difference increases with the increase in projectile energy till ionisation cross-sections reach maximum. σ_T obtained from this simple approximation has yielded reliable results in a number of targets studied [53–55].

The present scattering results (σ_I, σ_E and σ_T) for different amines are plotted in figures 1–9 where they are also compared with the available results. It is apparent that the obtained results are in good agreement with the available results at all energy values. The agreement is also excellent at low and intermediate energy range. For molecules like EA, propylamine (PA), butylamine (BA), DEA and TEA, collision data are not available for comparison. Hence, our results should serve as benchmark calculations for future studies. The numerical data of the cross-sections are provided in the supplementary material.

Some useful inferences are drawn based on the present calculations.

(A) The MA, EA, PA and BA form homologous chain of molecules and termed as family 1. Likewise, TMA and TEA form homologous family 2. The DMA and DEA form another homologous series termed as family 3. The collision from series of molecules has led to the following important observations.

(1) It is observed that the electronic spatial extent ($\langle R^2 \rangle$) of the target molecule increases with the molecular size characterised by N, the number of electrons. The radial spatial extent is a measure of the probable extent of electron charge density from the centre of charge. As we move away from the nuclei, this probability decreases
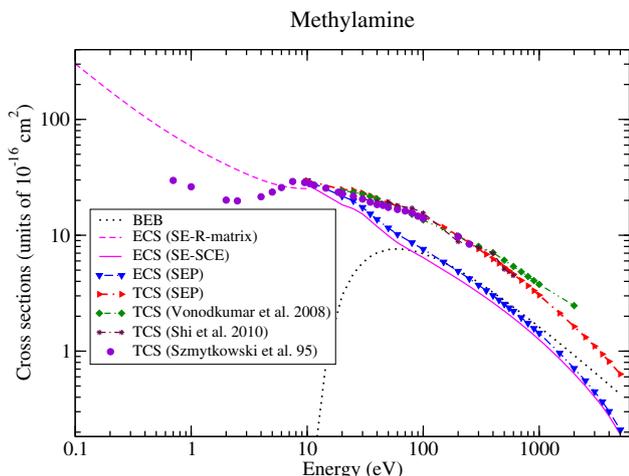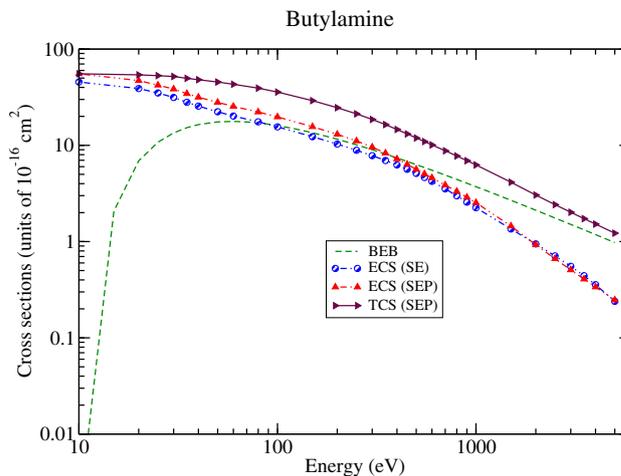
Figure 1. Cross-sections for e^--scattering from MA.
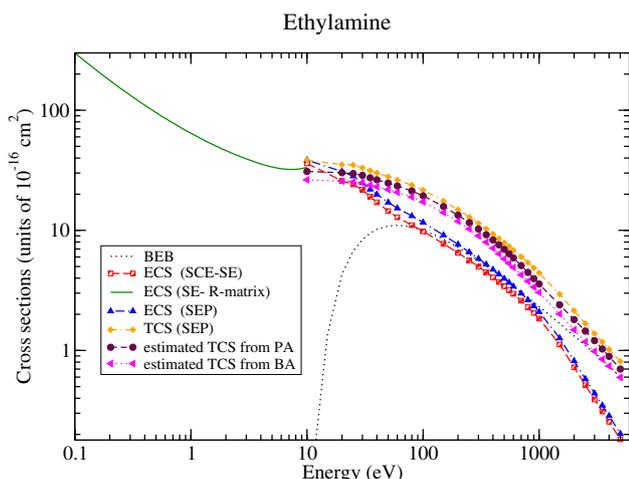
Figure 4. Cross-sections for e^--scattering from BA.

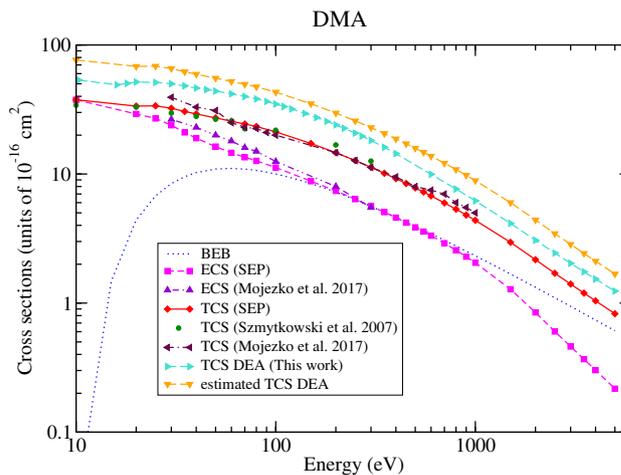**Figure 2.** Cross-sections for e^--scattering from EA.

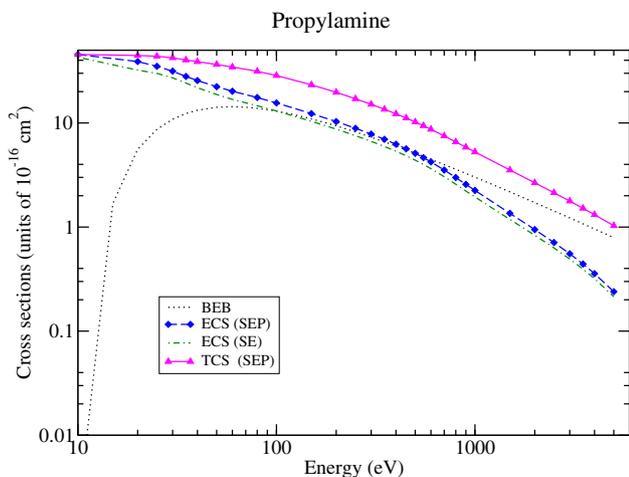**Figure 5.** Cross-sections for e^--scattering from DMA.
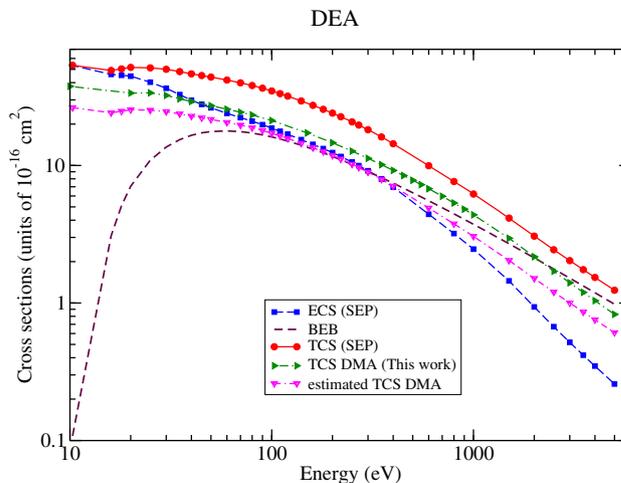
Figure 3. Cross-sections for e^--scattering from PA.
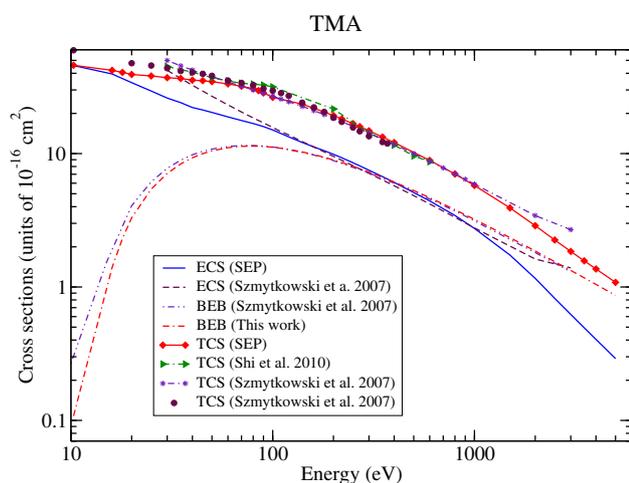
Figure 6. Cross-sections for e^--scattering from DEA.

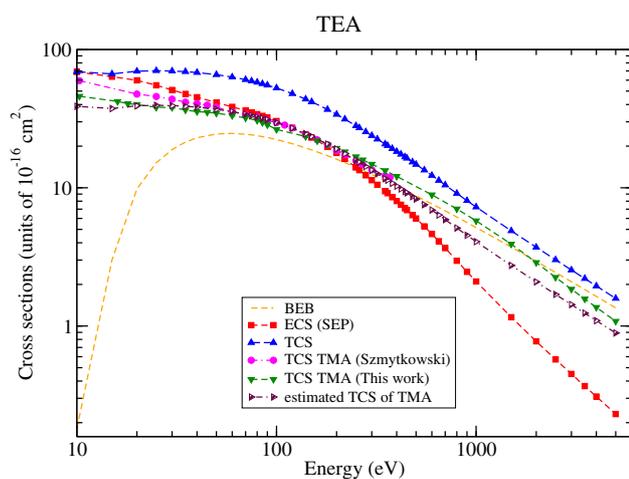**Figure 7.** Cross-sections for e^--scattering from TMA.

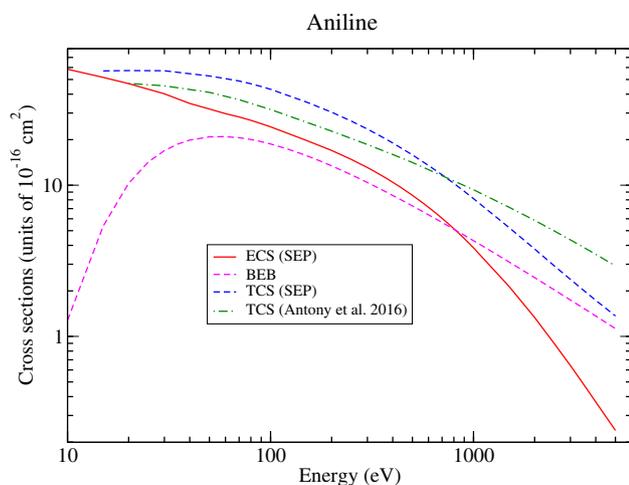**Figure 8.** Cross-sections for e^--scattering from TEA.

Figure 9. Cross-sections for e^--scattering from aniline.

sharply. Thus, the larger electronic spatial extent of a molecule offers greater electron–molecule interaction. This can be the reason for TCS to increase with $\langle R^2 \rangle$ for all molecules belonging to a particular homologous family. The value of $\langle R^2 \rangle$ for all molecules is mentioned in table 1.

2. The anisotropy of the molecule contributes significantly to TCS [38]. Incorporating the effects arising due to anisotropy and radial extent, a relationship is proposed between the TCS of any two molecules (X, Y) belonging to a particular homologous family

$$\sigma_{T(X)} = \sigma_{T(Y)} * N_Y * \langle R^2 \rangle_X / (N_X * \langle R^2 \rangle_Y). \quad (15)$$

In the most simple form, the anisotropy is expressed in terms of N, i.e., the total number of electrons. Using this equation, we estimated the TCS for molecules like MA and TMA for which experimental data are available. The estimated TCSs are shown in figures 10 and 8 respectively and appear to be in fair agreement with theoretical and experimental values. We have also used eq. (16) to estimate the TCS of other molecules belonging to families 1–3. These are shown in figures 2, 5 and 6. The estimated TCS for all molecules are close to the present theoretical values. This simple empirical formula can be a good tool to estimate the TCS data especially in cases where there is difficulty in performing the scattering calculations. This is also stressed by Fedus and Karwasz [56].

(B) To understand the effect of polarisation on scattering, in the energy regime considered, the calculations were also performed in SE approximation. It is observed that ECS obtained in SE and SEP models do not differ significantly for all targets. The representative scattering results are shown only for alkyl amines in figures 1–4. This holds good even for BA which has a very large polarisability of $90.29a_0^3$. It is likely that beyond the ionisation threshold, the interaction between the impinging electron and the target is very small to cause any distortion of molecular charge density. Both the models would yield identical scattering results in the asymptotic limit.

(C) It was natural to compare the low-energy results (below the ionisation threshold) obtained using the highly accurate R-matrix theory [57] with SCE results near the ionisation threshold. The SE is a unique model irrespective of the theory applied. It is therefore expected that SCE and R-matrix approaches should provide nearly the same values of ECS near the ionisation threshold in SE model. The representative calculations were therefore performed in SE model using the R-matrix and SCE approaches for MA and EA only. Nearly same values of cross-sections were obtained from the two approaches near the ionisation threshold as shown in figures 1 and 2, thus highlighting a smooth transition.
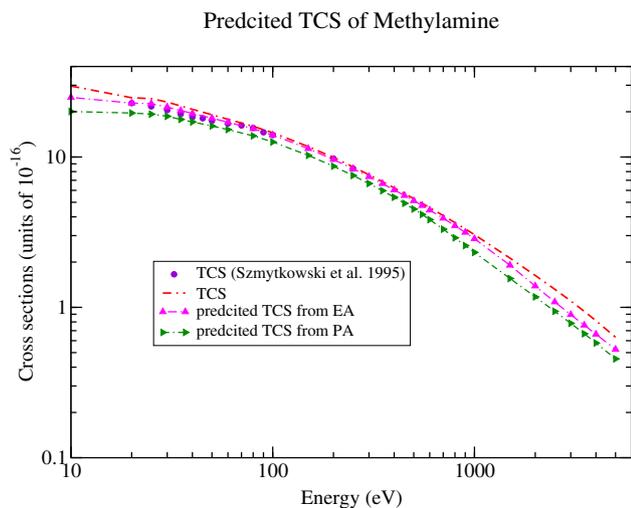
Predcited TCS of Methylamine

Figure 10. Estimated cross-sections for e^--scattering from MA.

Table 2. SE-ECS (10^{-16} cm^2) at 10 eV determined using R-matrix and SCE approaches.

Molecule	R-matrix	SCE
CH_3NH_2	25.33	27.47
$CH_3CH_2NH_2$	33.44	36.06

This means that both the methods can be combined to obtain the cross-sections from low to high energy. The SE results at 10 eV are tabulated in table 2 for representative molecules.

4. Conclusions

The continued emission of amines is bound to disturb the biosphere adversely. Electron-driven processes contribute not only to the development of advanced technologies but also to the fields of planetary physics and biology. Amines like MA and EA are essential precursors in the formation of amino acids in interstellar media. The understanding and modelling of electron-induced reactions require comprehensive sets of scattering data. Using SCE, we have obtained excellent results that match very well with the experimental data. The proposed semiempirical formulation gives reasonably accurate results. This formula may prove useful when it is difficult to perform calculations for any reason. The accurate cross-section data for various amines would help in devising efficient plasma reactors in pursuit of cleaner atmosphere. The smooth transition from R-matrix to SCE results suggest that the two methods can be combined to estimate the cross-sections from low to

high energy without any loss in accuracy. More coordinated efforts are required between molecular physicists, plasma chemists and environmentalist in developing an integrated approach to curtail the emission of amines into the atmosphere. We hope the present work would motivate experimentalists to take up the challenge and obtain the collision data of other molecular species.

References

[1] L Pereira, P K Mondal and M Alves, Aromatic amines sources, environmental impact and remediation, in: *Pollutants in buildings, water and living organisms* edited by E Lichtfouse, J Schwarzbauer and D Robert (Springer International, Berlin, 2015)
[2] X Ge, A S Wexler and S L Clegg, *Atmos. Environ.* **45**, 524 (2011)
[3] C J Tsai, M L Chen, A D Ye, M S Chou, S H Shen and I F Mao, *Atmos. Environ.* **42**, 8246 (2008)
[4] S Rappert and R Müller, *Waste Manag.* **25**, 887 (2005)
[5] S Sollinger and K Levsen, *Atmos. Environ.* **28**, 2369 (1994)
[6] Y Wang, J Zhang, A R Marcotte, M Karl, C Dye and P Herckes, *Atmos. Res.* **151**, 72 (2015)
[7] J Sintermann and A Neftel, *Biogeosciences* **12**, 3225 (2015)
[8] B Brunekreef and S T Holgate, *Lancet* **360**, 1233 (2002)
[9] J Ring, B Eberlein-Koenig and H Behrendt, *Ann. Allergy Asthma Immunol.* **87**, 2 (2001)
[10] K Donaldson, V Stone, A Seaton and W MacNee, *Environ. Health Perspect.* **109**, 523 (2001)
[11] H Duhme, S K Weiland and U Keil, *Toxicol. Lett.* **102**, 307 (1998)
[12] S M Murphy, A Sorooshian, J H Kroll, N L Ng, P Chhabra, C Tong, J D Surratt, E Knipping, R C Flagan and J H Seinfeld, *Atmos. Chem. Phys.* **7**, 2313 (2007)
[13] A A Assadi, J Palau, A Bouzaza, J Penya-Roja, V Martinez-Soriac and D Wolbert, *J. Photochem. Photobiol. A: Chem.***282**, 1 (2014)
[14] A A Assadi, A Bouzaza, M Lemasle and D Wolbert, *J. Photochem. Photobiol. A: Chem.* **282**, 18 (2014)
[15] W Tanthapanichakoon, P Khongprasarnkaln, T Charinpanitkul, H Tamon, N Sano and M Okazak, *ScienceAsia* **25**, 57 (1999)

[16] Z Ye, J Zhao, H Y Huang, F Ma and R Zhang, *J. Hazardous Mater*. **260**, 32 (2013)

[17] J Jolibois, K Takashima and A Mizuno, *J. Electrostat.* **70**, 300 (2012)

[18] F Ouni, A Khacef and J M Cormier, *Plasma Chem. Plasma Process*. **29**, 119 (2013)

[19] N Fourikis, K Takagi and M Morimoto, *Astrophys. J.* **191**, L139 (1974)

[20] D P Glavin, J P Dworkin and S A Sandford, *Met. Planet. Sci*. **43**, 399 (2008)

[21] N Kaifu, M Morimoto, K Nagane, K Akabane, T Iguchi and K Takagi, *Astrophys. J.* **191**, L135 (1974)

[22] S Muller, A Beelen, M Guelin, S Aalto, J H Black, F Combes, S Curran, P Theule and S Longmore, *Astron. Astrophys*. **535**, A103 (2011)

[23] M Förstel, A Bergantini, P Maksyutenko, S Gobi and R I Kaiser, *Astrophys. J.* **845**, 83 (2017)

[24] P D Gidfrey, R D Brown, B J Robinson and M W Sinclair, *Astrophys. J.* **13**, L119 (1973)

[25] P D Holtom, C J Bennett, Y Osamura, N J Mason and R I Kaiser, *Astrophys. J.* **626**, 940 (2005)

[26] C Szmytkowski and A M Krzysztofowicz, *J. Phys. B* **28**, 4291, 28 (1995)

[27] F M Silva, M H F Bettega and S Sanchez, *Eur. Phys. J. D* **68**, 12 (2014)

[28] M Vinodkumar, C Limbachiya, K N Joshipura, B Vaishnav and S Gangopadhyay, *J. Phys. Conf. Ser.* **115**, 012013 (2008)

[29] D Shi, J Sun and Z Zhu, *Eur. Phys. J. D* **57**, 179 (2010)

[30] C Szmytkowski, A Domaracka, P Możejko and E Ptasinska-Denga, *Phys. Rev. A* **75**, 052721 (2007)

[31] P Możejko, B Żywicka and A Domaracka, *IOP Conf. Ser.: J. Phys.: Conf. Ser.* **875**, 062048 (2017)

[32] S Singh, R Naghma, J Kaur and B Antony, *J. Chem. Phys*. **145**, 034309 (2016)

[33] F A Gianturco, D G Thompson and A K Jain, *Computational methods for electron molecule collisions* edited by W M Huo and F A Gianturco (Plenum, New York, 1995)

[34] F A Gianturco, R R Lucchese, N Sanna and A Talamo, A generalized single centre approach for treating electron scattering from polyatomic molecules, in: *Electron collisions with molecules, clusters, and surfaces* edited by H Ehrhardt and L A Morgan (Plenum, New York, 1994)

[35] S Hara, *J. Phys. Soc. Jpn*. **22**, 710 (1967)

[36] J P Perdew and A Zunger, *Phys. Rev. B* **23**, 5048 (1981)

[37] R Curik, F A Gianturco and N Sanna, *J. Phys. B* **33**, 2705 (2000)

[38] A Jain and F A Gianturco, *J. Phys. B* **24**, 2387 (1991)

[39] N Sanna and F A Gianturco, *Comput. Phys. Commun*. **128**, 139 (2000)

[40] A P P Natalense and R R Lucchese, *J. Chem. Phys*. **111**, 5344 (1999)

[41] F A Gianturco, R R Lucchese and N Sanna, *J. Chem. Phys*. **100**, 6464 (1994)

[42] Y K Kim, W Hwang, N M Weinberger, M A Ali and M E Rudd, *J. Chem. Phys*. **106**, 1026 (1997)

[43] N Sanna, I Baccarelli and G Morelli, *Comput. Phys. Commun*. **180**, 2544 (2009)

[44] GAUSSIAN 03, Gaussian, Inc, Wallingford, CT

[45] N Sanna and F A Gianturco, *Comput. Phys. Commun*. **114**, 142 (1998)

[46] Y H Jiang, J F Sun and L D Wan, *Phys. Rev. A* **62**, 062712 (2000)

[47] G Staszewska, D W Schwenke, D Thirumalai and D G Truhlar, *Phys. Rev. A* **28**, 2740 (1983)

[48] F Blanco and G García, *Phys. Rev. A* **67**, 022701 (2003).

[49] S Kaur, A Bharadvaja and K L Baluja, *Phys. Rev. A* **83**, 062707 (2011)

[50] A Bharadvaja, S Kaur and K L Baluja, *Phys. Rev. A* **87**, 062703 (2013)

[51] A Bharadvaja, S Kaur and K L Baluja, *Phys. Rev. A* **91**, 032701 (2015)

[52] A Bharadvaja, S Kaur and K L Baluja, *Pramana – J. Phys*. **89**: 30 (2017)

[53] A Bharadvaja, S Kaur and K L Baluja, *Phys. Plasmas* **26**, 063506 (2019)

[54] A Bharadvaja, S Kaur and K L Baluja, *Eur. Phys. J. D* **73**, 199 (2019)

[55] A Bharadvaja, S Kaur and K L Baluja, *Eur. Phys. J. D* **73**, 251 (2019)

[56] K Fedus and G Karwasz, *Eur. Phys. J. D* **71**, 138 (2017)

[57] J Tennyson, *Phys. Rep*. **491**, 29 (2010)

[58] NIST, Computational Chemistry Comparison and Benchmark DataBase, http://cccbdb.nist.gov

[59] D R Lide, *CRC Handbook of chemistry and physics*, 74 edn (CRC Press, Boca Raton, FL, 1993)